Materials Science & Engineering A 718 (2018) 43–47

Contents lists available at ScienceDirect

Materials Science & Engineering A

journal homepage: www.elsevier.com/locate/msea

Short communication

Influence of pre-strain on the gaseous hydrogen embrittlement resistance of a high-entropy alloy

Yakai Zhao[a], Dong-Hyun Lee[b], Woo-Jin Kim[b], Moo-Young Seok[c], Ju-Young Kim[d], Heung Nam Han[e], Jin-Yoo Suh[f,*], Upadrasta Ramamurty[g], Jae-il Jang[b,*]

[a] School of Materials Science and Engineering, Beijing Institute of Technology, Beijing 100081, China
[b] Division of Materials Science and Engineering, Hanyang University, Seoul 04763, Republic of Korea
[c] Max-Planck-Institut für Eisenforschung GmbH, Max-Planck-Straße 1, Düsseldorf 40237, Germany
[d] School of Materials Science and Engineering, Ulsan National Institute of Science and Technology, Ulsan 44919, Republic of Korea
[e] Department of Materials Science and Engineering, Seoul National University, Seoul 08826, Republic of Korea
[f] High Temperature Energy Materials Research Center, Korea Institute of Science and Technology, Seoul 02792, Republic of Korea
[g] Department of Materials Engineering, Indian Institute of Science, Bangalore 560012, India

ARTICLE INFO

Keywords:
High-entropy alloy
Hydrogen embrittlement
Pre-strain effect
Thermal desorption spectroscopy

ABSTRACT

The effect of pre-strain on the resistance to gaseous hydrogen embrittlement of CoCrFeMnNi high-entropy alloy (HEA) was investigated through mechanical testing and thermal desorption analysis. The results reveal that prior plastic deformation does not affect either the hydrogen contents or the excellent hydrogen embrittlement resistance of the HEA.

1. Introduction

High-entropy alloys (HEAs), which by definition comprise of at least five metallic constituent elements in (nearly-)equal amounts (in at%), have been attracting considerable attention in the recent past. This is because of their exceptional mechanical properties such as high specific strength combined with good ductility and excellent mechanical performance over a wide range of temperatures [1–5]. For future structural applications of HEAs, the influence of hydrogen (H) on their mechanical behavior is one of the crucial and essential topics of research since many potential applications of HEAs may lead to H exposure [6–8] and thus there is the possibility of hydrogen embrittlement, which could manifest as severe loss in ductility, unpredictable cracking that leads to premature fracture, and stress corrosion cracking [9–12]. Hence a close examination is warranted, but HEAs' resistance to hydrogen embrittlement was not examined in detail. As an early step of the research, very recently we explored the effect of H on the mechanical behavior of CoCrFeMnNi HEA (which is one of the most widely investigated HEAs to date [13–18]), by subjecting it to either electrochemical or gaseous charging [6,7]. The experimental results show that its resistance to gaseous hydrogen embrittlement is considerably more than face-centered cubic (fcc) austenitic stainless steels. This is in spite of HEA's strong ability to absorb H. We showed that higher hydrogen embrittlement resistance is due to the H content upon charging being below the threshold value for triggering the mechanism of H-enhanced localized plasticity (HELP) [7,9]. An important issue, which remains unaddressed, is the influence of H on the mechanical performance of *deformed* HEA, which is crucial for two reasons. First, any pre-straining can possibly change the microstructure and, in turn, affect the hydrogen embrittlement resistance. Second, most of structural metals experience some level of straining during the final step of manufacturing before being deployed. Here, it is worth noting that published data shows that such pre-strain accelerates the hydrogen embrittlement in austenitic stainless steels [19–21]. Keeping this in view, we examine the effects of pre-strain on the gaseous hydrogen embrittlement resistance of the CoCrFeMnNi HEA.

2. Experimental

The HEA samples were prepared by vacuum induction casting of nominal mixtures of the corresponding metals, each with a purity > 99 wt%. The cast ingot was hot-rolled and then solution annealed at 1100 °C for 1 h to reach an equilibrium state of single phase fcc microstructure. Four different levels of pre-strain (10%, 20%, 30%, and 40% true strain) were introduced by recourse to interrupted tensile tests on dog-bone-shaped plate-type samples with gauge length and width of 25 and 5 mm, respectively (following ASTM E8). Tests were performed under displacement rate control (1.5 mm/min) [4]. The

* Corresponding authors.
E-mail addresses: jinyoo@kist.re.kr (J.-Y. Suh), jijang@hanyang.ac.kr (J.-i. Jang).

https://doi.org/10.1016/j.msea.2018.01.107
Received 18 November 2017; Received in revised form 22 January 2018; Accepted 24 January 2018
Available online 31 January 2018
0921-5093/

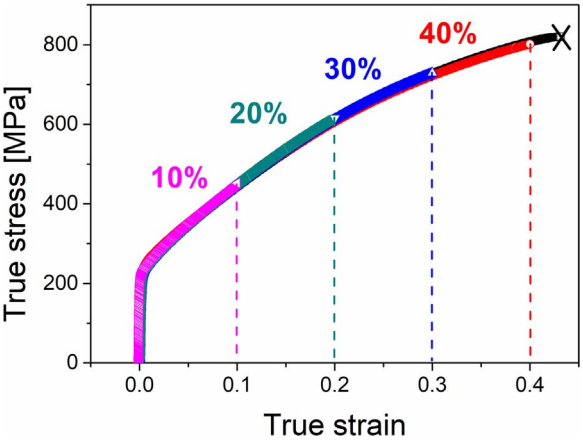

Fig. 1. The representative true stress-true strain curves obtained from the normal and interrupted tensile tests of CoCrFeMnNi HEA sample.

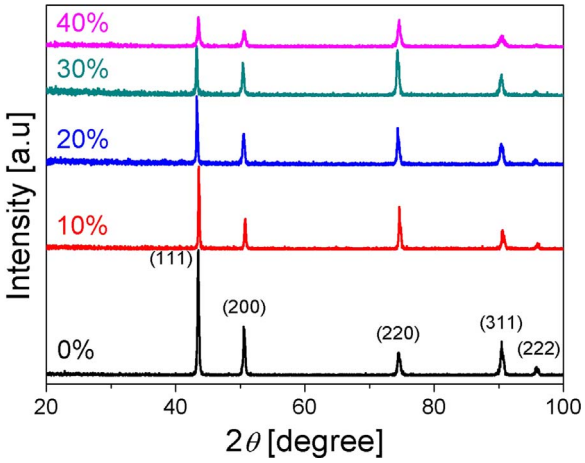

Fig. 2. The representative results from XRD.

tensile elongation (failure strain) of the uncharged sample was ~43% (as shown in Fig. 1) and uniform deformation was observed almost until the failure without necking. Note that such tensile tests with large-sized samples were only to prepare pre-strained samples but not directly for studying H effects.

Microstructure characterizations of the gauge parts of the interrupted samples were conducted by using X-ray diffraction (XRD; D/MAX-2500, Rigaku-Denki, Japan), electron backscattered diffraction (EBSD; CrystAlign system with the e-FlashHR detector, Bruker, Germany) mounted on a field emission scanning electron microscope (FE-SEM; S-4300SE, Hitachi, Japan), and transmission electron microscopy (TEM; Talos F200X, FEI Co., Hillsboro, OR, USA).

From the gauge parts of the interrupted specimens, sub-sized flat tensile specimens (with gauge length and width of 10 and 1 mm, respectively [7]) as well as small rectangular pieces were extracted, and were ground with colloidal silica (0.05 μm) to a mirror finish, resulting in a uniform thickness of ~300 μm. Gaseous H charging was performed on both sets of specimens in a custom-made Sieverts apparatus at 300 °C under a constant pressure of 15 MPa, which is the maximum capacity of the apparatus, for 72 h. This charging condition is known to be effective in evaluating the hydrogen-induced change in mechanical behavior of austenitic stainless steels [22,23] (that have the same fcc structure and similar main elements as CoCrFeMnNi HEA [3,7]). To minimize the influence of outgassing, all the charged samples were immediately immersion stored in liquid nitrogen until subsequent experiments, which were completed, in any case, within ~24 h after charging. Sub-sized tensile tests were carried out on both uncharged and charged samples using a micro-tensile tester (MTest 300, Gatan Inc., Pleasanton, CA, USA) at a cross-head speed of 0.1 mm/mm (which corresponds to an initial strain rate of $\sim 1.7 \times 10^{-4}\ s^{-1}$). Nanoindentation experiments were conducted on the rectangular samples using Nanoindenter-XP (formerly MTS; now Keysight Technologies, Santa Rosa, CA, USA) equipped with a Berkovich indenter. All the indentation tests were performed to a peak load, P_{max}, of 100 mN with constant indentation strain rate, $\dot{\varepsilon} = (dh/dt)/h = 0.025\ s^{-1}$ where h is indentation depth and t is time. For the quantitative analysis of the H content in the charged rectangular samples, thermal desorption spectroscopy (TDS) was performed with a quadrupole mass spectroscope (EX0014, R-DEC Company, Tsukuba, Japan) at a constant heating rate of 5 °C/min to the maximum temperature of ~800 °C.

3. Results and discussion

The true stress vs. true strain response of the HEA, superposed with those obtained from the interrupted tensile tests, is displayed in Fig. 1. After yielding at a stress, σ_y, of ~220 MPa, the HEA exhibits considerable work hardening before failing at a stress of ~820 MPa and 43% strain.

The microstructural characterization of the pre-strained specimens was performed with XRD, EBSD, and TEM. In all the XRD scans (Fig. 2), identical peak positions, all of which correspond to a single fcc phase, confirm the absence of stress induced phase transformation [8,15,24]. The lattice parameters estimated (~3.591–3.594 Å) are well within the reported range (3.59–3.61 Å [25–27]) for this HEA. Microstructural analysis performed with EBSD and TEM, Fig. 3a and b, shows only a few annealing twins and low dislocation density in the unstrained sample. Upon straining to 20%, grain distortion and a significant increase in dislocation density within the grains [28] were noted. Further straining to 40% leads to elongation of the grains along the tensile direction; the grains are almost filled with highly tangled dislocations, which is in agreement with the prior reports on HEAs [29,30].

Results of the micro-tensile tests performed on the 0–40% pre-strained HEA samples before and after gaseous H charging are displayed in Fig. 4, from which the following two observations can be made. (a) H charging does not affect the strain hardening behavior and the ductility of the HEA in any significant manner. (b) In 0% and 20% strained samples, H charging does not seem to affect σ_y whereas it slightly increases in samples strained to 30% and above. Laplanche et al. [30] estimated the threshold stress for the initiation of mechanical twinning in the same HEA as ~720 ± 30 MPa. Fig. 4 indicates that σ_y in samples strained to 30% and beyond is either similar or higher to this value. Since H is known to reduce the stacking fault energy, which, in turn, promotes twinning [31,32], the H-induced slight strengthening observed in highly pre-strained HEA samples is possibly due to pronounced development of mechanical twinning [8].

Variations in the hardness, estimated by using the Oliver-Pharr method [33] on the nanoindentation data, with pre-strain are plotted in Fig. 5 for both before- and after-charging conditions. From it, we noted that H charging does not alter the hardness in any substantial manner at all pre-strain levels. The absence of a significant hardness increase in 30% and 40% pre-strained samples (unlike the results of tensile tests, especially for 40% pre-strained samples) may be explained by the differences in stress condition and deformation size between nanoindentation and micro-tensile tests; i.e., the stress condition underneath an indenter is much more complex than that in a uniaxial tensile sample, and the deforming volume during the nanoindentation is much smaller than that in the tensile tests of micro-sized (but still bulky) samples. Combined with the possibility that twinning may prefer some grains (having specific orientations) and deformation mode, these differences may suppress the increase in local hardness.

In an earlier study [7], we observed that gaseous charging of H does not embrittle CoCrFeMnNi HEA and thus rationalized it on the basis that the local H content being below a certain threshold level required

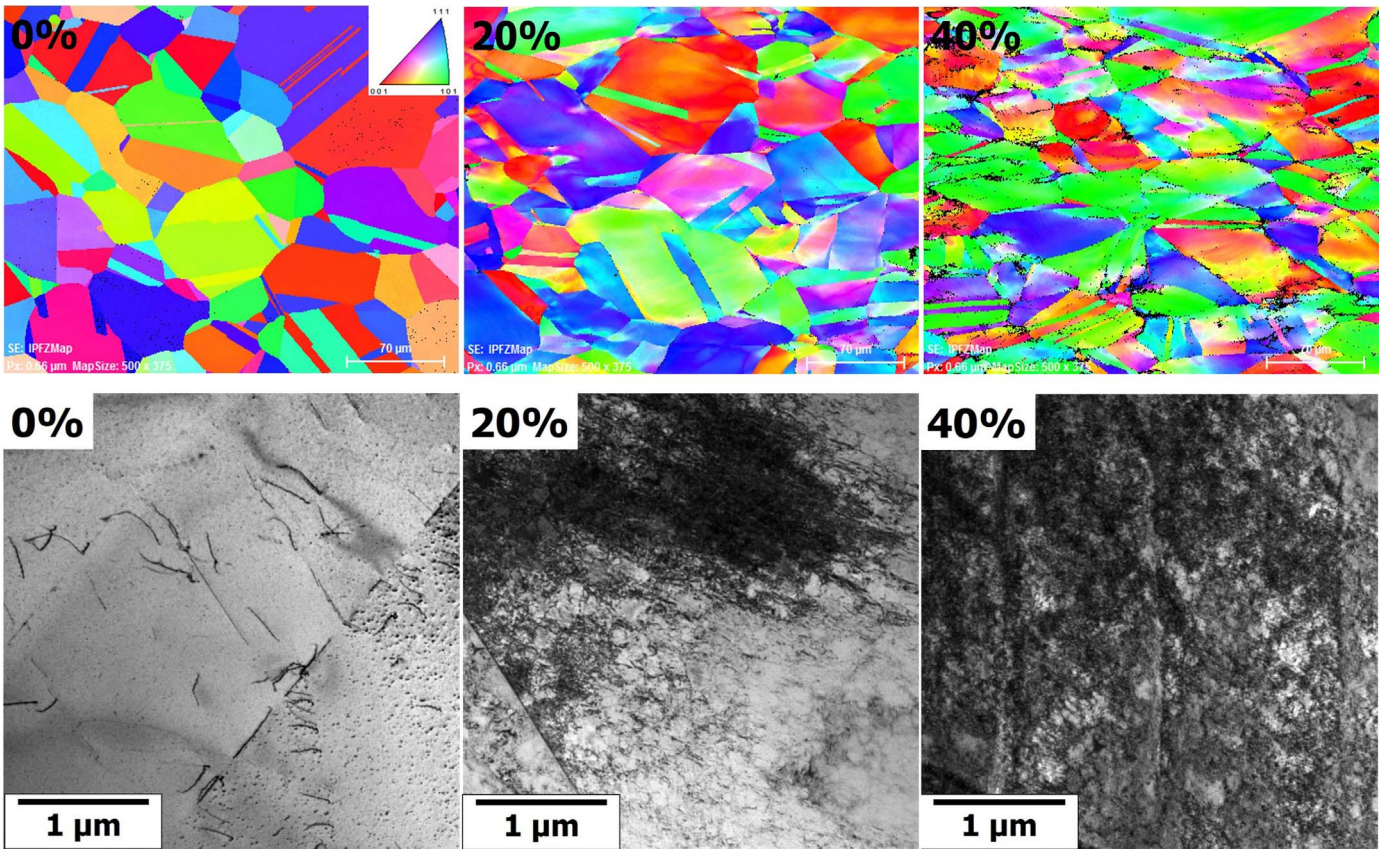

Fig. 3. Microstructural evolution in the pre-strained samples; the representative results from (a) EBSD, and (c) TEM.

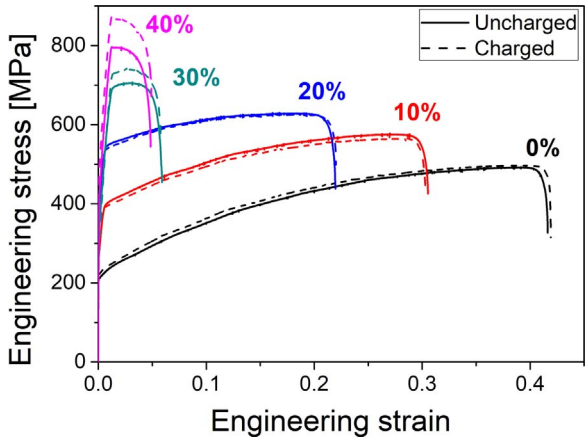

Fig. 4. Typical engineering stress-engineering strain curves from micro-tensile tests.

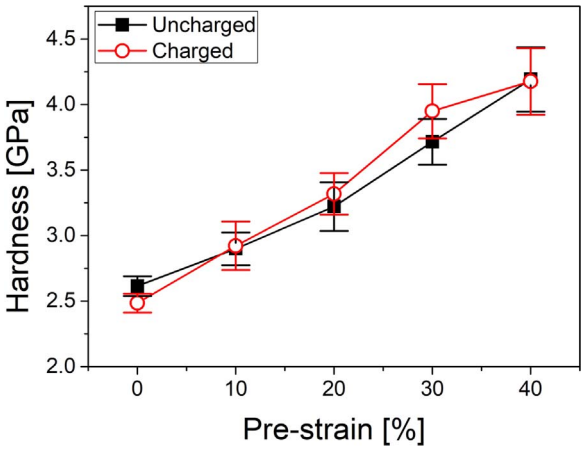

Fig. 5. Variation in nanoindentation hardness with pre-strain.

for triggering HELP. The results of the present study, in particular the invariance of ductility in pre-strained and H charged samples, further establish the excellent resistance of the HEA under investigation to gaseous H embrittlement. In addition, they imply that pre-straining does not significantly alter the threshold H levels for triggering the HELP mechanism.

The H content in the pre-strained samples after charging were measured by analyzing TDS curves, and the results are displayed in Fig. 6. The H content of the annealed sample is ~63.2 wppm that is at a similar level to that reported in previous study, ~76.5 wppm [7], confirming the reason for the hydrogen embrittlement resistance being insufficient H content as discussed above. Two features of Fig. 6 are noteworthy. Pre-straining does not appear to alter the temperature of the peak desorption. This observation implies that the main H trapping sites remain unaltered by the pre-straining. More importantly, the H content, which is given by the area under the desorption curve, is not significantly affected by pre-straining. This indicates that the largely increased dislocation density in the pre-strained samples did not enhance the capacity of the HEA to absorb H, which is what one would expect as dislocations are known to be effective H trapping sites [34–36]; an increase in dislocation density with plastic strain should have lead to larger amounts of trapped H. On the contrary, the H content in deformed samples is lower (by ~8.5–10.5 wppm) than that in the undeformed sample; possible reasons for this are discussed in the next paragraph. We can conclude that the lower H in the deformed HEA is the reason for the sustained good hydrogen embrittlement in them.

Results presented in Fig. 6 suggest that dislocations in the HEAs do not favor H atom trapping, unlike in conventional alloys. A plausible

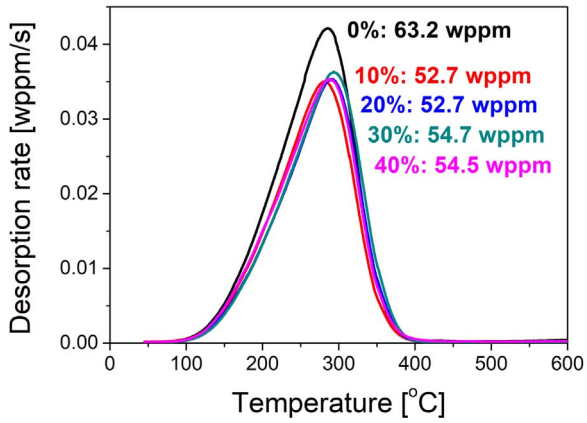

Fig. 6. H desorption curves obtained from TDS measurements of H-charged specimens.

reason for this may be the significant lattice strain energy [1,37] of HEAs, which is also one of the reasons for the high H solubility in CoCrFeMnNi HEA lattice [7]. Since the TDS peak temperatures, and thus the main H trapping sites, are not significantly affected by pre-straining (see Fig. 6), we can conclude it is the lattice rather than dislocations that continues to trap H. In this sense, "cleaner" microstructure of the annealed HEA sample than the pre-strained samples may explain a slightly higher H content in the former than in the latter; that is, probably less H atoms are expected to be trapped in dislocations than in HEA lattice. Recently, Zhao and Nieh [38] suggested that the CoCrFeMnNi HEA has a smaller dislocation core than pure Ni, which, in turn, may not favor preferential H segregation to dislocation cores [39]. Another possible contributing factor is the nanoscale heterogeneity such as co-clusters and/or short-range orders (SROs) that may exist in the lattice of CoCrFeMnNi HEA [40–42]. This is partially supported by the planar dislocation slip characteristics in CoCrFeMnNi HEA [29,30] since SRO typically suppresses cross-slip. Such nanoscale heterogeneities may favor H trapping and thus, at least partially, explain the high H solubility of annealed HEA. Plastic deformation leads to shearing of those co-clusters and SROs, and a reduction in their population [42] could lead to a reduced H solubility.

4. Conclusion

To summarize, the effect of prior-plastic deformation on the gaseous hydrogen embrittlement of CoCrFeMnNi HEA was investigated, results of which show that the excellent resistance of the HEA to hydrogen embrittlement is unaffected by pre-strains. This is because pre-straining does not enhance the H solubility in the HEA. On the contrary, it decreases the H solubility slightly due to the smaller dislocation core and the existence of nanoscale heterogeneity in the HEA that make the lattice more suitable for H atoms' occupation than dislocations.

Acknowledgements

The work at Hanyang University was supported by the National Research Foundation of Korea (NRF) grants funded by the Ministry of Science and ICT (No. 2015R1A5A1037627 and No. 2017R1A2B4012255). The work at KIST was supported by the Convergence Agenda Program (CAP) of the Korea Research Council of Fundamental Science and Technology. The authors wish to thank Han-Jin Kim (KIST) for his valuable supports with experiments.

Prime novelty statement

- Effect of pre-strain on hydrogen embrittlement resistance of high-entropy alloy was studied.
- Prior plastic deformation does not affect the excellent hydrogen embrittlement resistance of CoCrFeMnNi alloy.
- High-entropy alloy lattice may be more suitable hydrogen-trapping sites than dislocations.

References

[1] Y. Zhang, T.T. Zuo, Z. Tang, M.C. Gao, K.A. Dahmen, P.K. Liaw, Z.P. Lu, Microstructures and properties of high-entropy alloys, Prog. Mater. Sci. 61 (2014) 1–93.
[2] Y.F. Ye, Q. Wang, J. Lu, C.T. Liu, Y. Yang, High-entropy alloy: challenges and prospects, Mater. Today 19 (2016) 349–362.
[3] D.B. Miracle, O.N. Senkov, A critical review of high entropy alloys and related concepts, Acta Mater. 122 (2017) 448–511.
[4] H.Y. Diao, R. Feng, K.A. Dahmen, P.K. Liaw, Fundamental deformation behavior in high-entropy alloys: an overview, Curr. Opin. Solid State Mater. Sci. 21 (2007) 252–266.
[5] Z. Wu, M.C. Troparevsky, Y.F. Gao, J.R. Morris, G.M. Stocks, H. Bei, Phase stability, physical properties and strengthening mechanisms of concentrated solid solution alloys, Curr. Opin. Solid State Mater. Sci. 21 (2017) 267–284.
[6] Y. Zhao, D.-H. Lee, J.-A. Lee, W.-J. Kim, H.N. Han, U. Ramamurty, J.-Y. Suh, J.-i. Jang, Hydrogen-induced nanohardness variations in a CoCrFeMnNi high-entropy alloy, Int. J. Hydrog. Energy 42 (2017) 12015–12021.
[7] Y. Zhao, D.-H. Lee, M.-Y. Seok, J.-A. Lee, M.P. Phaniraj, J.-Y. Suh, H.-Y. Ha, J.-Y. Kim, U. Ramamurty, J.-i. Jang, Resistance of CoCrFeMnNi high-entropy alloy to gaseous hydrogen embrittlement, Scr. Mater. 135 (2017) 54–58.
[8] H. Luo, Z. Li, D. Raabe, Hydrogen enhances strength and ductility of an equiatomic high-entropy alloy, Sci. Rep. 7 (2017) 9892.
[9] H.K. Birnbaum, P. Sofronis, Hydrogen-enhanced localized plasticity—a mechanism for hydrogen-related fracture, Mater. Sci. Eng. A 176 (1994) 191–202.
[10] A. Barnoush, H. Vehoff, Recent development in the study of hydrogen embrittlement: hydrogen effect on dislocation nucleation, Acta Mater. 58 (2010) 5274–5285.
[11] I.M. Robertson, P. Sofronis, A. Nagao, M.L. Martin, S. Wang, D.W. Gross, K.E. Nygren, Hydrogen embrittlement understood, Metall. Mater. Trans. A 26 (2015) 2323–2341.
[12] G.S. Was, D. Farkas, I.M. Robetson, Micromechanics of dislocation channeling in intergranular stress corrosion nucleation, Curr. Opin. Solid State Mater. Sci. 16 (2012) 134–142.
[13] B. Cantor, I.T.H. Chang, P. Knight, A. Vincent, Microstructural development in equiatomic multicomponent alloys, Mater. Sci. Eng. A 375–377 (2004) 213–218.
[14] B. Gludovatz, A. Hohenwarter, D. Catoor, E.H. Chang, E.P. George, R.O. Ritchie, A fracture-resistant high-entropy alloy for cryogenic applications, Science 345 (2014) 1153–1158.
[15] B. Gludovatz, E.P. George, R.O. Ritchie, Processing, microstructure and mechanical properties of the CrMnFeCoNi high-entropy alloy, JOM 67 (2015) 2262–2270.
[16] D.-H. Lee, I.-C. Choi, M.-Y. Seok, J. He, Z. Lu, J.-Y. Suh, M. Kawasaki, T.G. Langdon, J.-i. Jang, Nanomechanical behavior and structural stability of a nanocrystalline CoCrFeNiMn high-entropy alloy processed by high-pressure torsion, J. Mater. Res. 30 (2015) 2804–2815.
[17] D.-H. Lee, M.-Y. Seok, Y. Zhao, I.-C. Choi, J. He, Z. Lu, J.-Y. Suh, U. Ramamurty, M. Kawasaki, T.G. Langdon, J.-i. Jang, Spherical nanoindentation creep behavior of nanocrystalline and coarse-grained CoCrFeMnNi high-entropy alloys, Acta Mater. 109 (2016) 314–322.
[18] D.-H. Lee, J.-A. Lee, Y. Zhao, Z. Lu, J.-Y. Suh, J.-Y. Kim, U. Ramamurty, M. Kawasaki, T.G. Langdon, J.-i. Jang, Annealing effect on plastic flow in nanocrystalline CoCrFeMnNi high-entropy alloy: a nanomechanical analysis, Acta Mater. 140 (2017) 443–451.
[19] Y. Mine, C. Narazaki, K. Murakami, S. Matsuoka, Y. Murakami, Hydrogen transport in solution-treated and pre-strained austenitic stainless steels and its role in hydrogen-enhanced fatigue crack growth, Int. J. Hydrog. Energy 34 (2009) 1097–1107.
[20] L. Zhang, Z. Li, J. Zheng, Y. Zhao, P. Xu, C. Zhou, X. Li, Effect of strain-induced martensite on hydrogen embrittlement of austenitic stainless steels investigated by combined tension and hydrogen release methods, Int. J. Hydrog. Energy 38 (2013) 8208–8214.
[21] H. Ji, I.-J. Park, S.-M. Lee, Y.-K. Lee, The effect of pre-strain on hydrogen embrittlement in 310S stainless steel, J. Alloy. Compd. 598 (2014) 205–212.
[22] M. Hatano, M. Fujinami, K. Arai, H. Fujii, M. Nagumo, Hydrogen embrittlement of austenitic stainless steels revealed by deformation microstructures and strain-induced creation of vacancies, Acta Mater. 67 (2014) 342–353.
[23] M.P. Phaniraj, Han-Jin Kim, Jin-Yoo Suh, Jae-Hyeok Shim, Seong-Jun Park, Tae-Ho Lee, Hydrogen embrittlement in high interstitial alloyed 18Cr10Mn austenitic stainless steels, Int. J. Hydrog. Energy 40 (2015) 13635–13642.
[24] F. Otto, N.L. Hanold, E.P. George, Microstructural evolution after thermomechanical processing in an equiatomic, single-phase CoCrFeMnNi high-entropy alloy with special focus on twin boundaries, Intermetallics 54 (2014) 39–48.
[25] W.H. Liu, Y. Wu, J.Y. He, T.G. Nieh, Z.P. Lu, Grain growth and the Hall-Petch relationship in a high-entropy FeCrNiCoMn alloy, Scr. Mater. 68 (2013) 526–529.
[26] C. Zhu, Z.P. Lu, T.G. Nieh, Incipient plasticity and dislocation nucleation of FeCoCrNiMn high-entropy alloy, Acta Mater. 61 (2013) 2993–3001.
[27] N.D. Stepanov, D.G. Shaysultanov, G.A. Salishchev, M.A. Tikhonovsky, E.E. Oleynik, A.S. Tortika, O.N. Senkov, Effect of V content on microstructure and mechanical properties of the CoCrFeMnNiV$_x$ high entropy alloys, J. Alloy. Compd. 628 (2015) 170–185.
[28] S.-H. Joo, H. Kato, M.J. Jang, J. Moon, C.W. Tsai, J.W. Yeh, H.S. Kim, Tensile

deformation behavior and deformation twinning of an equimolar CoCrFeMnNi high-entropy alloy, Mater. Sci. Eng. A 689 (2017) 122–133.
[29] F. Otto, A. Dlouhý, Ch Somsen, H. Bei, G. Eggeler, E.P. George, The influences of temperature and microstructure on the tensile properties of a CoCrFeMnNi high-entropy alloy, Acta Mater. 61 (2013) 5743–5755.
[30] G. Laplanche, A. Kostka, O.M. Horst, G. Eggeler, E.P. George, Microstructure evolution and critical stress for twinning in the CrMnFeCoNi high-entropy alloy, Acta Mater. 118 (2016) 152–163.
[31] A.E. Pontini, J.D. Hermida, X-ray diffraction measurement of the stacking fault energy reduction induced by hydrogen in an AISI 304 steel, Scr. Mater. 37 (1997) 1831–1837.
[32] M. Wen, S. Fukuyama, K. Yokogawa, Hydrogen-affected cross-slip in fcc nickel, Phys. Rev. B 69 (2004) 174108–174113.
[33] W.C. Oliver, G.M. Pharr, An improved technique for determining hardness and elastic modulus using load and displacement sensing indentation experiments, J. Mater. Res. 7 (1992) 1564–1583.
[34] A.J. Kumnick, H.H. Johnson, Deep trapping states for hydrogen in deformed iron, Acta Mater. 28 (1980) 33–39.
[35] M. Nagumo, K. Ohta, H. Saitoh, Deformation induced defects in iron revealed by thermal desorption spectroscopy of tritium, Scr. Mater. 40 (1999) 313–319.
[36] K.-i. Ebihara, T. Iwamoto, Y. Matsubara, H. Yamada, T. Okamura, W. Urushihara, T. Omura, Numerical analysis of influence of hydrogen charging method on thermal desorption spectra for pre-strained high-strength steel, ISIJ Int. 54 (2014) 153–159.
[37] M. Komarasamy, N. Kumar, R.S. Mishra, P.K. Liaw, Anomalies in the deformation mechanism and kinetics of coarse-grained high entropy alloy, Mater. Sci. Eng. A 654 (2016) 256–263.
[38] Y.Y. Zhao, T.G. Nieh, Correlation between lattice distortion and friction stress in Ni-based equiatomic alloys, Intermetallics 86 (2017) 45–50.
[39] A. Pundt, R. Kirchheim, Hydrogen in metals: microstructural aspects, Annu. Rev. Mater. Res. 36 (2006) 555–608.
[40] C. Niu, A.J. Zaddach, A.A. Oni, X. Sang, J.W. Hurt III, M.M. LeBeau, C.C. Koch, D.L. Irving, Spin-driven ordering of Cr in the equiatomic high entropy alloy NiFeCrCo, Appl. Phys. Lett. 106 (2015) 161906.
[41] Z. Wu, Y. Gao, H. Bei, Thermal activation mechanisms and Labusch-type strengthening analysis for a family of high-entropy and equiatomic solid-solution alloys, Acta Mater. 120 (2016) 108–119.
[42] S.I. Hong, J. Moon, S.K. Hong, H.S. Kim, Thermally activated deformation and the rate controlling mechanism in CoCrFeMnNi high entropy alloy, Mater. Sci. Eng. A 682 (2017) 569–576.